in *Computational Methods in Catalysis and Materials Science*, part of the IDECAT Course book series, Philippe Sautet and Rutger A. van Santen, editors (Wiley-VCH: 2008). Maximum 25 pages single spaced.

Contents

Chapter 1

TDDFT for Excited States

Mark E. Casida
Laboratoire de Chimie Théorique,
Département de Chimie Molécularie (DCM, UMR CNRS/UJF 5250),
Institut de Chimie Moléculaire de Grenoble (ICMG, FR2607),
Université Joseph Fourier (Grenoble I),
301 rue de la Chimie, BP 53,
F-38041 Grenoble Cedex 9, FRANCE
e-mail: Mark.Casida@UJF-Grenoble.Fr

Abstract: Since its introduction into quantum chemistry a little over a decade ago, linear response time-dependent density-functional theory (LR-TDDFT) has become a method of choice for the calculation of the electronic excited states of medium- and large-sized molecules. This chapter describes the formal basis and mathematics underlying conventional LR-TDDFT and illustrates its use through an application to the photochemical ring opening of oxirane.

1.1 Introduction

It may come as a surprise to younger researchers that DFT (density-functional theory) was once considered a "four letter word" by many traditional *ab initio* quantum chemists. The same younger researchers may also be surprised to learn that, even while DFT was being increasingly accepted in the early 1990s, it was still widely regarded as a firmly grounded principle that DFT could not handle excited states. Those attitudes have mostly changed. Typical modern quantum chemistry practice is now to use DFT where once Hartree-Fock (HF) was used to model the energy landscape and electronic properties of chemical systems, only carrying out HF calculations when needed as a starting point for sophisticated and costly *ab initio* many-body calculations. Moreover time-dependent DFT (TDDFT) has become, with few exceptions, the primary single-reference method for treating excited states in medium and large sized molecules, leading to a veritable explosion of publications over the past decade. The main objective of this chapter is answer the question "What is TDDFT?" by describing the formalism and mathematics behind modern "conventional" TDDFT. Some illustrations of the performance of the method will be given for the small molecule oxirane.

The use of TDDFT to treat electronic excited states is only about a decade old. Although several ideas had been put forth to deal with the excited-state problem[1], the fact remained that the original Hohenberg-Kohn theorems were for the ground state only and there was not yet any widely-accepted way to treat excited states in quantum chemistry using DFT. This changed rapidly in the

mid-1990s due in large part to an article entitled: "Time-dependent density-functional response theory for molecules" [2]. That article sent important messages to both the then still fairly separate DFT quantum chemistry and *ab initio* quantum chemistry communities. It explained to the DFT community that linear response theory could be used to reformulate TDDFT to resemble configuration interaction (CI) and hence to handle automatically configuration mixing in excited states. It explained to the *ab initio* community about the history and formal underpinnings of TDDFT, particularly the Runge-Gross theorems, [3] and hence justified the adaptation of recently developed technology for DFT second analytic derivatives to calculate excitation spectra using a formalism which very much resembled linear response time-dependent Hartree-Fock (LR-TDHF, also known as RPA for random phase approximation). Our own paper [4] and that of Bauernschmitt and Ahlrichs [5] soon confirmed that the method could give excellent excitation energies. Since then, LR-TDDFT has become part of virtually all quantum chemistry programs and many quantum physics programs around the world.

That TDDFT is an "unfinished subject" is attested to by the many variants which continue to appear, including but not limited to time-dependent current density-functional theory[6, 7], propagator corrections [8, 9, 10], spin-flip theory[11, 12, 13], range-separated hybrids[14, 15, 16, 17], and subsystem theory [18, 19, 20, 21]. In line with with these developments, many review articles on TDDFT have now appeared [22, 23, 2, 24, 25, 26, 27, 28, 29, 30, 31, 32, 33, 34, 35, 36, 35, 37, 38, 39], each emphasizing a somewhat different aspect of TDDFT. Given the vastness of the subject, some choices have had to be made as to what aspects to present here. I have decided to emphasize those aspects which I think are of most interest to quantum chemists, namely the calculation of excitation spectra and the treatment of excited-states potential energy surfaces (PESs.)

1.2 Formalism

Time-dependent density-functional theory (TDDFT) has its roots in ordinary ground-state density-functional theory (DFT). This section presents the basic formalism of both exact DFT and exact TDDFT and says a few words about approximate functionals.

1.2.1 Ground-state formalism

Before looking at the time-dependent problem, it is useful to begin with the time-independent (or static) problem. After the usual Born-Oppenheimer separation, the N-electron hamiltonian, $\hat{H}$, of the time-independent Schrödinger equation,

$$\hat{H}\Psi_I = E_I\Psi_I \; ; \; E_0 \leq E_1 \leq \cdots \, , \tag{1.1}$$

can be separated, $\hat{H} = \hat{T} + \hat{V}_{ee} + \hat{V}_{ext}$, into a kinetic energy term, $\hat{T}$, the electron-electron repulsion, $\hat{V}_{ee}$, and the external potential, $\hat{V}_{ext} = \sum_{i=1}^{N} v_{ext}(\mathbf{r}_i)$, representing the interaction of the electrons with the electric field of the nuclei and/or some other applied potential.

The objective of DFT is to avoid having to solve the N-electron Schrödinger equation (1.1) and working with complicated N-electron wave functions, by working with a simpler entity, namely the ground-state charge density,

$$\rho(\mathbf{r}_1) = N \int\int\cdots\int |\Psi_0(\mathbf{x}_1, \mathbf{x}_2, \mathbf{x}_3, \cdots, \mathbf{x}_N)|^2 \, d\sigma_1 d\mathbf{x}_2 d\mathbf{x}_3 \cdots d\mathbf{x}_N \, , \tag{1.2}$$

where $\mathbf{x}_i = (\mathbf{r}_i, \sigma_i)$ is shorthand for the space and spin coordinates of electron i. That we can do this at all is the somewhat surprising content of the two Hohenberg-Kohn theorems[40].

The first Hohenberg-Kohn theorem (HK1) tells us that the ground-state charge density determines the external potential up to an arbitrary additive constant: $\hat{V}_{ext} + C \leftarrow \rho$. (If desired, this constant can be fixed after the fact for finite systems by requiring that the potential goes to zero at infinite distance.) Since integrating the charge density gives the number of electrons, HK1 tells us that the hamiltonian is also determined up to an arbitrary additive constant: $\hat{H} + C \leftarrow \rho$. So the ground-state charge density fixes just about everything, including the excitation energies,

$$\hbar\omega_I = E_I - E_0 \,, \tag{1.3}$$

and their associated oscillator strengths,

$$f_I = \frac{2m_e\omega_I}{3\hbar} \sum_{q=x,y,z} |\langle\Psi_0|q|\Psi_I\rangle|^2 \,. \tag{1.4}$$

That is ρ determines the molecule's stick spectrum [41]. Thus both ground- and excited-state properties are functionals of the ground-state density, but we do not know these more general functionals [42].

The second Hohenberg-Kohn theorem (HK2) tells us that there is a variational principle for the ground-state energy,

$$E_0 \leq F[\rho] + \int v_{ext}(\mathbf{r})\rho(\mathbf{r})\, d\mathbf{r} \,, \tag{1.5}$$

with equality only if ρ is a ground-state charge density (degenerate ground states are allowed.) The functional, F, is universal in the sense that it is independent of v_{ext}. It is *not* unknown because it may be written explicitly as,

$$F[\rho] = \min_{\Psi \to \rho} \frac{\langle\Psi|\hat{T} + \hat{V}_{ee}|\Psi\rangle}{\langle\Psi|\Psi\rangle} \,, \tag{1.6}$$

This constrained variational form [43] is important for a number of reasons, including the facts that it eliminates the original Kohn-Sham v-representability assumption (i.e., that the trial densities can be realized as the ground state of some system) and applies to degenerate ground states. However it is far from practical since it implies carrying out a calculation even more difficult than full configuration interaction (CI.) Thus simplifying approximations are still required if the Hohenberg-Kohn variational principle is to become practical.

These simplifications are aided by the Kohn-Sham reformulation of DFT [44]. A fictitious system of noninteracting electrons,

$$\left[-\frac{\hbar^2}{2m_e}\nabla^2 + v_s(\mathbf{r})\right]\psi_i(\mathbf{r}) = \epsilon_i\psi_i(\mathbf{r}) \,, \tag{1.7}$$

is considered with N occupied orthonormal orbitals which generate the same charge density as that of the interacting system: $\rho(\mathbf{r}) = \sum_i n_i|\psi_i(\mathbf{r})|^2 \leftarrow \Phi_s$. Here the n_i are orbital occupation numbers, and v_s and Φ_s are respectively the Kohn-Sham single-particle potential and the Kohn-Sham determinant made from the N occupied orbitals. The total energy may now be written in a form reminiscent of the HF model,

$$E_{KS} = -\frac{\hbar^2}{2m_e}\sum_i n_i\langle\psi_i|\nabla^2|\psi_i\rangle + \int v_{ext}(\mathbf{r})\rho(\mathbf{r})\, d\mathbf{r} + \frac{1}{2}\int\int \frac{\rho(\mathbf{r}_1)\rho(\mathbf{r}_2)}{r_{12}}\, d\mathbf{r}_1 d\mathbf{r}_2 + E_{xc}[\rho] \,, \tag{1.8}$$

where the exchange-correlation (xc) energy is given by,

$$E_{xc}[\rho] = \min_{\Psi \to \rho} \frac{\langle\Psi|\hat{T} + \hat{V}_{ee}|\Psi\rangle}{\langle\Psi|\Psi\rangle} - \min_{\Phi_s \to \rho} \frac{\langle\Phi_s|\hat{T}|\Phi_s\rangle}{\langle\Phi_s|\Phi_s\rangle} - \frac{1}{2}\int\int \frac{\rho(\mathbf{r}_1)\rho(\mathbf{r}_2)}{r_{12}}\, d\mathbf{r}_1 d\mathbf{r}_2 \,, \tag{1.9}$$

Table 1.1: Jacob's ladder for functionals.

Quantum Chemical Heaven		
double-hybrid	——	$\rho_\sigma(\mathbf{r}), x_\sigma(\mathbf{r}), \tau_\sigma(\mathbf{r}), \psi_{i\sigma}(\mathbf{r}), \psi_{a\sigma}(\mathbf{r})^d$
hybrid	——	$\rho_\sigma(\mathbf{r}), x_\sigma(\mathbf{r}), \tau_\sigma(\mathbf{r}), \psi_{i\sigma}(\mathbf{r})^c$
mGGA	——	$\rho_\sigma(\mathbf{r}), x_\sigma(\mathbf{r}), \tau_\sigma(\mathbf{r})^b$
GGA	——	$\rho_\sigma(\mathbf{r}), x_\sigma(\mathbf{r})^a$
LDA	——	$\rho_\sigma(\mathbf{r})$
Hartree World		

[a] The reduced gradient $x_\sigma(\mathbf{r}) = |\vec{\nabla}\rho_\sigma(\mathbf{r})|/\rho_\sigma^{4/3}(\mathbf{r})$.
[b] The local kinetic energy $\tau_\sigma(\mathbf{r}) = \sum_i n_{i\sigma}\psi_{i\sigma}(\mathbf{r})\nabla^2\psi_{i\sigma}(\mathbf{r})$.
[c] Occupied orbitals.
[d] Unoccupied orbitals.

and contains not only exchange and correlation but also the difference between the kinetic energies of the real interacting and fictitious noninteracting systems. Minimizing the Kohn-Sham energy subject to the constraint of orthonormal orbitals gives Eq. (1.7), but with $v_s(\mathbf{r}) = v_{ext}(\mathbf{r}) + v_{xc}(\mathbf{r})$, where the xc-potential is the functional derivative [45] of the xc-energy,

$$v_{xc}(\mathbf{r}) = \frac{\delta E_{xc}[\rho]}{\delta\rho(\mathbf{r})}\,. \tag{1.10}$$

The success of applied DFT is due to the quality of available approximations for the xc-energy. Reviewing all of these approximations would be a chapter in and of itself and so we refer the reader to other works for a more complete treatment [46, 47]. However we do need to say a few words here about some of the approximations because of their use in TDDFT calculations. (Indeed, TDDFT has proven to be one of the driving horses behind developping new functionals.)

Improvements in functionals come in two different but complementary ways. One is to make the functional form more exact without changing the variables on which the functional depends. The other approach to increase the number of variables on which the functional depends. This latter approach consists of climbing the Jacob's ladder shown in Table 1.1. While adding more variables should, in principle, make it easier to design more reliably accurate functionals, all that is really guaranteed in climbing the ladder is that calculations will become more expensive. Hence it is also important to improve the functionals at the lower ends of the ladder.

The very first expansion of the variable list has been to include a dependance on the two densities $\rho_\uparrow$ and $\rho_\downarrow$, rather than the total density, ρ. This extension is so common place that DFT is commonly understood to mean spin DFT and we will follow this practice. The local density approximation (LDA) and generalized gradient approximations (GGAs) are examples of pure density functionals since they are orbital-dependent. They were the traditional workhorses of DFT until Axel Becke proposed the use of hybrid functionals [48] including a fraction of orbital-dependent Hartree-Fock exchange on the basis of adiabatic connection theory and to improve the accuracy of DFT for thermochemistry. Hybrids are often found to lead to increased accuracy in TDDFT calculations, but are computationally more expensive. Meta-GGAs (mGGAs) are a step down the ladder and in the level of computational difficulty in that the orbital dependence is limited to calculating the

local kinetic energy. Recently Stephane Grimme and Frank Neese have moved up the ladder by recommending a double-hybrid of the form,

$$E_{xc}^{double-hybrid} = a_x E_x^{HF} + (1-a_x)E_x^{GGA} + a_c E_c^{GGA} + (1-a_c)E_c^{MP2}\,, \tag{1.11}$$

for applications in TDDFT, where E_x^{HF} is the HF exchange energy, E_x^{GGA} and E_c^{GGA} are respectively GGA exchange- and correlation-energy functionals, and E_c^{MP2} is the second-order Møller-Plesset (MP2) energy [49].

A problem with hybrid functionals is that the xc-potential is no longer a "simple" multiplicative function as intended in the original Kohn-Sham theory. Following Sharp and Horton [50] and Talman and Shadwick [51], insight into the behavior of the exact exchange potential can be obtained by seeking the optimized effective potential (OEP) whose orbitals minimize the HF energy. The answer [50] turns out to be that this is equivalent to asking that the linear reponse of the DFT charge density to the perturbation $(\hat{\Sigma}_x^\sigma - v_x^\sigma)$ be zero. While exact solutions are possible [51], Krieger, Li, and Iafrate, following up on a footnote in the Sharp-Horton paper [50], found a very successful approximate solution [52]:

$$v_x^\sigma(\mathbf{r}) = \frac{\sum_i n_{i\sigma}\psi_{i\sigma}^*(\mathbf{r})\hat{\Sigma}_x^\sigma\psi_{i\sigma}(\mathbf{r})}{\rho_\sigma(\mathbf{r})} + \frac{\sum_i n_{i\sigma}(\epsilon_{i\sigma}^{DFT} - \epsilon_{i\sigma}^{HF})|\psi_{i\sigma}(\mathbf{r})|^2}{\rho_\sigma(\mathbf{r})}\,, \tag{1.12}$$

where ρ_σ is the spin σ charge density, the HF exchange operator, $\hat{\Sigma}_x^\sigma$, acts by $\hat{\Sigma}_x^\sigma\phi(\mathbf{r}_1) = -\int(\gamma_\sigma(\mathbf{r}_1,\mathbf{r}_2)/r_{12})\phi(\mathbf{r}_2)\,d\mathbf{r}_2$, and $\gamma_\sigma(\mathbf{r}_1,\mathbf{r}_2) = \sum_i \psi_{i\sigma}(\mathbf{r}_1)n_{i\sigma}\psi_{i\sigma}^*(\mathbf{r})$, is the one-electron reduced density matrix (1-RDM or just "density matrix.") The first term in Eq. (1.12) is Slater's form of v_x^σ while the second term is a derivative discontinuity term which leads to sudden rigid jumps in the potential when new orbitals are occupied. At large r only the HOMO of each spin contributes, leading, after a bit of algebra, to,

$$v_x^\sigma(\vec{r}) = -\frac{1}{r} + \epsilon_{HOMO}^{DFT} - \epsilon_{HOMO}^{HF}\,. \tag{1.13}$$

We now see that the HOMO energy must be the same in DFT and HF if the x-potential vanishes at infinity. This is a reflection of the general theorem that $-\epsilon_{HOMO}^{DFT}$ must be the ionization potential when the xc-functional is exact. The exact xc-potential must fall off as $-1/r$ at large distances.

Figure 1.1 shows orbital energies obtained from our own exchange-only OEP calculations [53]. It turns out that minus the Kohn-Sham orbital energy is a remarkably good approximation to the corresponding ionization potential. In fact, the graphic shows a dramatic improvement in Koopmans' theorem when the HF exchange operator is transformed into a localized exchange potential by the OEP procedure. The behavior of the unoccupied orbitals can be understood by using a result of Gonze and Scheffler obtained from an exchange-only time-dependent OEP theory [54]. (See also my own article [10] for an alternative approximate demonstration.) The result is that,

$$\epsilon_a^{DFT} = \epsilon_a^{HF} - (\epsilon_i^{HF} - \epsilon_i^{DFT}) - (aa|f_H|ii) - (ai|f_{xc}^{\uparrow,\uparrow}(\epsilon_a - \epsilon_i)|ia)\,. \tag{1.14}$$

Here the indices include spin and

$$(pq|f|rs) = \int\int \psi_p^*(\mathbf{r})\psi_q(\mathbf{r})f(\mathbf{r},\mathbf{r}')\psi_r^*(\mathbf{r}')\psi_s(\mathbf{r}')\,d\mathbf{r}d\mathbf{r}'\,, \tag{1.15}$$

where f can be either the Hartree kernel,

$$f(\mathbf{r}_1,\mathbf{r}_2) = 1/r_{12}\,, \tag{1.16}$$

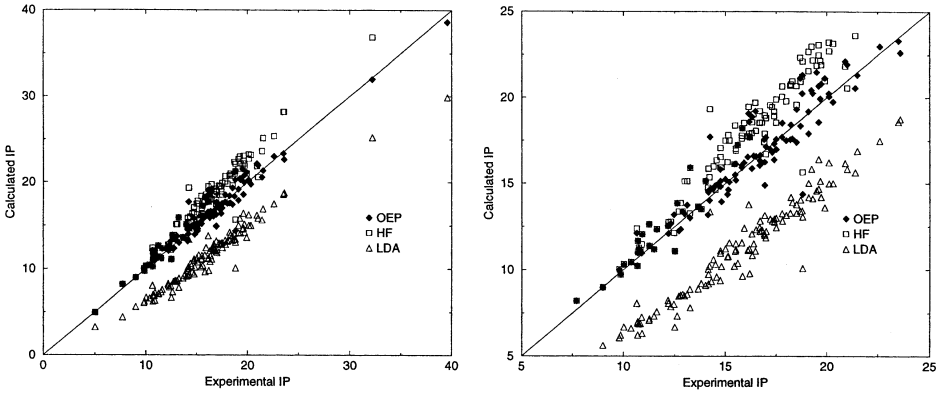

(a) All. (b) Enlargement.

Figure 1.1: Correlation between minus the OEP ($\diamond$), HF (filled square), and LDA ($\triangle$) orbital energies and experimental outer valence ionization potentials for 26 small molecules and a total of over 100 ionization potentials. [53].

or the xc-kernel which is given by,

$$f_{xc}^{\sigma,\tau}(\mathbf{r}_1,\mathbf{r}_2) = \frac{\delta^2 E_{xc}[\rho_\uparrow,\rho_\downarrow]}{\delta\rho_\sigma(\mathbf{r}_1)\delta\rho_\tau(\mathbf{r}_2)}\,, \tag{1.17}$$

in the adiabatic approximation. Ignoring the small frequency dependence of f_{xc} and choosing i to be the HOMO, we obtain,

$$\epsilon_a^{DFT} = \epsilon_a^{HF} - (aa|f_H|ii) - (ai|f_{xc}^{\uparrow,\uparrow}|ia)\,. \tag{1.18}$$

This latter equation has a simple interpretation. Unoccupied HF orbitals see N electrons while unoccupied KS orbitals see the same potential as occupied KS orbitals, hence $(N-1)$ electrons. To go from the HF case to the DFT case, it is therefore necessary to remove a coulomb integral and an exchange integral. Practical experience suggests that the answer should be roughly independent of the occupied orbital i as long as the orbital is not too localized.

Potentials from approximate pure density functionals do not behave like Eq. (1.12). They do not show the sudden jump (or "derivative discontinuity") which arises from the second term when a new orbital is populated and the long-range behavior of the xc-potentials is also different. Since charge densities fall off exponentially at large r, the LDA exchange potential ($v_x^\sigma = -C_x\rho_\sigma^{4/3}$) also falls off exponentially at large r which is too rapidly in comparison with the correct $1/r$ behavior. Also since the exchange part dominates the correlation part, this leads to underbinding not only in the LDA but also in GGAs, hence to HOMOs which are too small in magnitude by as much as 5 eV in typical small molecules. One way to correct this is to introduce model potentials [55, 56, 57] which fall off asymptotically as $1/r$ for exponentially decaying charge densities. However the resulting xc-potentials are no longer the functional derivative of an xc-energy functional. Hybrid functionals do lead to "potentials" with improved asymptotic behavior, behaving as a constant times $1/r$ at long distances. The short-range/long-range separated hybrid functionals appear to give even better results in this respect. [14, 15, 16, 17]

1.2.2 Time-dependent formalism

We now turn our attention to the time-dependent version of Eq. (1.1), namely

$$\hat{H}\Psi(t) = i\hbar\frac{\partial}{\partial t}\Psi(t)\,. \tag{1.19}$$

Modern TDDFT is based upon two theorems of Runge and Gross (RG1 and RG2) [3] which are the analogues of the two Hohenberg-Kohn theorems (HK1 and HK2).

The first theorem is fundamentally a theorem about the current density,

$$\mathbf{j}(\mathbf{r}_1,t) = \frac{N\hbar}{m_e}\Im m\left\{\int\int\cdots\int\left[\nabla_1\Psi(\mathbf{x}_1,\mathbf{x}_2,\cdots,\mathbf{x}_N,t)\right]\Psi^*(\mathbf{x}_1,\mathbf{x}_2,\cdots,\mathbf{x}_N,t)\,d\sigma_1 d\mathbf{x}_2\cdots d\mathbf{x}_N\right\}\,. \tag{1.20}$$

The current density satisfies the continuity equation,

$$\frac{\partial\rho(\mathbf{r},t)}{\partial t} + \nabla\cdot\mathbf{j}(\mathbf{r},t) = 0\,. \tag{1.21}$$

In the case of a single-determinant wave function, $\vec{j}(\mathbf{r},t) = (\hbar/m_e)\Im m\sum_{i=1,N}\left[\nabla\psi_i(\mathbf{r},t)\right]\psi_i^*(\mathbf{r},t)\,.$

RG1 states that the time-dependent charge-density determines the external potential up to an additive function of time: $v_{ext}(\mathbf{r},t) + C(t) \leftarrow \rho(\mathbf{r},t)\,.$ It is assumed that the external potential can be expressed as a Taylor series in time, $v_{ext}(\mathbf{r},t) = \sum_{k=0}^{\infty} c_k(\mathbf{r})(t-t_0)^k$ with $c_k(\mathbf{r}) = (1/k!)\left[\partial^k v_{ext}(\mathbf{r},t)/\partial t^k\right]_{t=t_0}$. Most physical potentials can be approximated arbitrarily closely by such a function. The equation of motion,

$$i\hbar\frac{\partial\langle\Psi(t)|\hat{j}_q|\Psi(t)\rangle}{\partial t}(t) = \langle\Psi(t)|\left[\hat{j}_q,\hat{H}(t)\right]|\Psi(t)\rangle\,, \tag{1.22}$$

is used to show that two external potentials generating the same current density cannot differ by more than an additive function of time. Then the continuity equation (1.21) is used to show from this result that two external potentials generating the same time-dependent charge density cannot differ by more than an additive function of time. This involves the vanishing of a certain integral over a boundry surface which will always be the case for normal electric fields generated by finite sets of charges. A corollary to RG1 is that the time-dependent charge density, $\rho(\mathbf{r},t)$, fixes the number of particles, N, and the external potential up to an arbitrary additive function of time, $v_{ext}(\mathbf{r},t)+C(t)$. Hence $\rho(\mathbf{r},t)$ determines the time-dependent hamiltonian up to an additive function of time: $\hat{H}(t) + C(t) \leftarrow \rho(\mathbf{r},t)\,.$ That means that the equation of motion for the wave function can always be integrated provided we know the initial wave function, Ψ_0, at time t_0 to obtain, $\Psi(t) = \Psi[\rho,\Psi_0](t)e^{i\phi(t)}\,.$ where the phase factor is given by, $\phi(t) = \int_{t_0}^{t} C(t')\,dt'\,.$ If our system is in its ground state at time t_0, then we can use HK1 to remove the dependence on Ψ_0 to obtain, $\Psi(t) = \Psi[\rho](t)e^{i\phi(t)}\,.$

Thanks to RK1 we have that the external potential of the real system is a functional of the density. This is also true for the fictitious system of noninteracting electrons, so we can write down a time-dependent Kohn-Sham equation,

$$\left[-\frac{1}{2}\nabla_1^2 + v_{ext}(\mathbf{r}_1,t) + \int\frac{\rho(\mathbf{r}_2,t)}{r_{12}}\,d\mathbf{r}_2 + v_{xc}[\rho](\mathbf{r}_1,t)\right]\psi_i(\mathbf{r}_1,t) = i\hbar\frac{\partial\psi_i(\mathbf{r}_1,t)}{\partial t}\,. \tag{1.23}$$

The goal of RG2 was to propose a stationary action principle in analogue to the variational principle of HK2. This will not be discussed here except to note that the Dirac-Frenkel action, $A =$

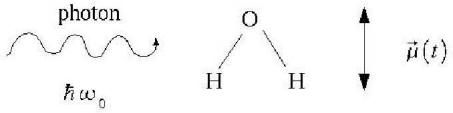

Figure 1.2: A water molecule perturbed by a photon. The photon is modeled by a classical time-dependent electric field. We are interested in the induced dipole moment which is also a function of time.

$\int_{t_0}^{t_1} \langle \Psi(t') | i\hbar \frac{\partial}{\partial t'} - \hat{H}(t') | \Psi(t') \rangle \, dt'$, originally proposed by Runge and Gross proved to be inadequate. It was replaced by Robert van Leeuwen with a more appropriate Keldysh action formalism[27].

Almost all applications of TDDFT make the adiabatic approximation which assumes that the xc-potential reacts instantaneously and without memory to any temporal change in the charge density. Then

$$v_{xc}[\rho](\mathbf{r}, t) = \frac{\delta E_{xc}[\rho_t]}{\delta \rho_t(\mathbf{r})} \,, \tag{1.24}$$

where $\rho_t(\mathbf{r})$ is a function of $\mathbf{r} = (x, y, z)$ obtained by fixing t in the function $\rho(\mathbf{r}, t)$. The result is expected. The time-independent Kohn-Sham equation has been transformed into a time-dependent Kohn-Sham equation by replacing the orbital energy with a time-derivative, making the orbitals time-dependent, and inserting the time-dependent charge density wherever the density appears.

Only a little is known about how to go beyond the adiabatic approximation. Perhaps the most successful approach has been the Vignale-Gross formalism which includes nonadiabatic effects through the current density[6, 7]. Another approach involves a comoving Lagrangian reference frame[58]. More recently work has been carried out to extract the nonadiabatic behavior of the xc-kernel from the Bethe-Salpeter equation via a polarization propagator formalism[8, 9, 10].

1.3 Technology

At this point the reader may be wondering how we are going to extract excitation energies from TDDFT. The answer is that we are going to make a textbook application of linear response theory which will completely eliminate time in favor of excitation energies. This section describes important mathematical "technology" needed to go from the formal theory described in the previous section to obtain excited-state quantities of interest in quantum chemistry.

1.3.1 Formal Response Theory

Consider a time-dependent perturbation applied to a molecule initially in its ground stationary state. We would like to express the response of a property to this perturbation in terms of the states of the unperturbed system. An important example is shown in Fig. 1.2. Other examples include NMR chemical shifts and circular dichroism spectra.

We assume that the exact solution is known for the Schrödinger equation for the unperturbed system (molecule.) The time-independent equation was given in Eq. (1.1). The corresponding time-dependent equation is,

$$\hat{H}\Psi_I(t) = i\hbar \frac{\partial}{\partial t} \Psi_I(t) \,, \tag{1.25}$$

with, $\Psi_I(t) = \Psi_I e^{-iE_I t/\hbar}$. (Careful! The notation is compact: $\Psi_I(t) \neq \Psi_I$.)

Now apply the time-dependent perturbation, $\hat{b}(t)$. The equation governing the time evolution of the perturbed system is, $\left(\hat{H} + b(t)\right)\Psi_0(t) = i\hbar\partial\Psi_0(t)/\partial t$. Without loss of generality, $\Psi_0(t) = (\Psi_0 + \delta\Psi_0(t) + \cdots)\, e^{-iE_0 t/\hbar}$, which allows us to deduce that the linear response of the ground state, $\delta\Psi_0(t)$, satisfies the first-order equation,

$$\hat{b}(t)\Psi_0\left(i\hbar\frac{\partial}{\partial t} - \hat{H} + E_0\right) = \hat{b}(t)\Psi_0\delta\Psi_0(t)\,. \tag{1.26}$$

After an appropriate Fourier transform, this first-order equation is just,

$$\left[E_0 - \hat{H} + \hbar\omega\right]\delta\Psi_0(\omega) = \hat{b}(\omega)\Psi_0\,, \tag{1.27}$$

which is very nice because this equation is now in the usual form for applying Rayleigh-Schrödinger perturbation theory. We can immediately write down that,

$$\delta\Psi_0(\omega) = \sum_{I\neq 0}\Psi_I\frac{\langle\Psi_I|\hat{b}(\omega)|\Psi_0\rangle}{\hbar(\omega-\omega_I)}\,, \tag{1.28}$$

where $\hbar\omega_I$ is the Ith excitation energy of the unperturbed system [Eq. (1.3).]

In order to go further, we assume that the perturbation is monochromatic, so $\hat{b}(t) = b\cos(\omega_0 t)$ and $\hat{b}(\omega) = \pi b\left[\delta(\omega+\omega_0) + \delta(\omega-\omega_0)\right]$. Inserting into Eq. (1.28) and back Fourier transforming gives,

$$\delta\Psi_0(t) = \left[\sum_{I\neq 0}\Psi_I\frac{\omega_I\langle\Psi_I|\hat{b}|\Psi_0\rangle}{\hbar(\omega_0^2-\omega_I^2)}\right]\cos(\omega_0 t) - i\left[\sum_{I\neq 0}\Psi_I\frac{\omega_0\langle\Psi_I|\hat{b}|\Psi_0\rangle}{\hbar(\omega_0^2-\omega_I^2)}\right]\sin(\omega_0 t)\,. \tag{1.29}$$

The linear response, $\delta\langle\hat{a}\rangle(t) = \langle\Psi_0|\hat{a}|\delta\Psi_0(t)\rangle + \langle\delta\Psi_0(t)|\hat{a}|\Psi_0\rangle$, of an observable, a, is given by,

$$\delta\langle\hat{a}\rangle(t) = \left[\sum_{I\neq 0}\frac{2\omega_I\Re e(\langle\Psi_0|\hat{a}|\Psi_I\rangle\langle\Psi_I|\hat{b}|\Psi_0\rangle)}{\hbar(\omega_0^2-\omega_I^2)}\right]\cos(\omega_0 t) + \left[\sum_{I\neq 0}\frac{2\omega_0\Im m(\langle\Psi_0|\hat{a}|\Psi_I\rangle\langle\Psi_I|\hat{b}|\Psi_0\rangle)}{\hbar(\omega_0^2-\omega_I^2)}\right]\sin(\omega_0 t)\,. \tag{1.30}$$

This result is very powerful. We see that the response to a perturbation at frequency ω_0 is at the same frequency. The phase is also the same if the operators $\hat{a}$ and $\hat{b}$ are both real (polarizability) or both imaginary (NMR). The phase is $\pi/2$ if one of $\hat{a}$ and $\hat{b}$ is real and the other is imaginary (circular dichroism.)

We finally arrive at the point where we will specialize to the case of the electric polarizability. The dynamic polarizability is the proportionality tensor between the linear response of the dipole moment, μ, and the applied field, $\mathcal{E}_q(t) = \mathcal{E}_q\cos(\omega t)$, namely

$$\mu_q(t) = \mu_q + \sum_{q'=x,y,z}\alpha_{q,q'}(\omega)\mathcal{E}_{q'}\cos(\omega t) + \cdots\ ;\ q = x,y,z\,. \tag{1.31}$$

For us, the dynamic polarizability will be a way to access excited states. At optical frequencies, the variation in the electric field is too rapid for the nuclei to follow, so we may consider them clamped in place. The response of the dipole moment is then entirely electronic and we may write,

$$\begin{aligned}\delta\mu_q(t) &= -e\langle\Psi_0|q|\delta\Psi_0(t)\rangle - e\langle\delta\Psi_0(t)|q|\Psi_0\rangle \\ &= \sum_{q'=x,y,z}\left[\sum_{I\neq 0}\frac{2e^2\omega_I\Re e(\langle\Psi_0|q|\Psi_I\rangle\langle\Psi_I|q'|\Psi_0\rangle)}{\hbar(\omega_I^2-\omega^2)}\right]\mathcal{E}_{q'}\cos(\omega t)\,.\end{aligned} \tag{1.32}$$

The quantity in square brackets is $\alpha_{q,q'}(\omega)$. As we often do not know the orientation of the molecules, it is the average dynamic polarizability,

$$\alpha(\omega) = \sum_{I\neq 0} \frac{e^2 f_I}{m_e(\omega_I^2 - \omega^2)}\,, \tag{1.33}$$

which is important. The oscillator strengths, f_I, are defined in Eq. (1.4). Equation (1.33) is known as the sum-over-states (SOS) theorem and relates the dynamic response of the density to the excited states.

1.3.2 LR-TDDFT

So far, we have assumed that we know the exact wave function solution of the unperturbed problem for the interacting system. This is not known in DFT, so some modifications are necessary. The result are the basic equations for linear-response TDDFT (LR-TDDFT). The approach taken here is based upon density matrices[2]. In what follows, "DFT" means "pure DFT." As the result for linear-response time-dependent Hartree-Fock (LR-TDHF) is also given, it is trivial to write down the corresponding generalization for hybrid functionals.

In HF and in DFT the density matrix of the unperturbed system is,

$$\gamma_\sigma(\mathbf{r},\mathbf{r}') = \sum \psi_{p\sigma}(\mathbf{r}) P_{pq\sigma} \psi_{p\sigma}(\mathbf{r}')\ ;\ P_{pq\sigma} = n_{p\sigma}\delta_{p,q}\,. \tag{1.34}$$

Its response to a time-dependent electric field is, $\delta\gamma_\sigma(\mathbf{r},\mathbf{r}') = \sum \psi_{p\sigma}(\mathbf{r})\delta P_{pq\sigma}(\omega)\psi^*_{q\sigma}(\mathbf{r}')$. As

$$\delta\psi_{i\sigma}(\mathbf{r}\omega) = \sum_p \psi_{p\sigma}(\mathbf{r}) \frac{\langle\psi_{p\sigma}|\hat{b}(\omega)|\psi_{i\sigma}\rangle}{\omega - (\epsilon_{p\sigma} - \epsilon_{i\sigma})}\,, \tag{1.35}$$

and as, $\delta\gamma_\sigma(\mathbf{r},\mathbf{r}') = \sum_i \delta\psi_{i\sigma}(\mathbf{r}) n_i \psi^*_{i\sigma}(\mathbf{r}') + \sum_i \psi_{i\sigma}(\mathbf{r}) n_i \delta\psi^*_{i\sigma}(\mathbf{r}')$, then,

$$\delta P_{pq\sigma}(\omega) = \frac{n_{q\sigma} - n_{p\sigma}}{\omega - (\epsilon_{p\sigma} - \epsilon_{q\sigma})} \langle\psi_{p\sigma}|\hat{b}_{eff}(\omega)|\psi_{q\sigma}\rangle\,, \tag{1.36}$$

for $\hat{b}(t) = \hat{b}\cos(\omega t)$.

The reason for writing $\hat{b}_{eff}(\omega)$ and not just $\hat{b}(\omega)$ is that $\hat{b}_{eff}(\omega)$ is the perturbation felt by the HF or DFT orbitals and not the applied field. The difference between these two perturbations is the response of the self-consistent field, $\hat{b}_{eff}(\omega) = \hat{b}(\omega) + \delta\hat{v}_{SCF}(\omega)$. In terms of matrices,

$$b^{eff}_{pq\sigma}(\omega) = b_{pq\sigma}(\omega) + \sum K_{pq\sigma,rs\tau}\delta P_{rs\tau}(\omega)\,, \tag{1.37}$$

where the coupling matrix is,

$$K_{pq\sigma,rs\tau} = \frac{\partial v^{SCF}_{pq\sigma}}{\partial P_{rs\tau}} = \begin{cases} (pq|f_H|rs) - \delta_{\sigma,\tau}(pr|f_H|sq) & ;\quad \text{HF} \\ (pq|f_H|rs) + (pq|f^{\sigma,\tau}_{xc}|rs) & ;\quad \text{DFT} \end{cases}\,. \tag{1.38}$$

Note that we have made the adiabatic approximation, even if this is not strictly necessary [2]. Thus we have that

$$\delta P_{pq\sigma}(\omega) = \frac{n_{q\sigma} - n_{p\sigma}}{\omega - (\epsilon_{p\sigma} - \epsilon_{q\sigma})} \left[b_{pq\sigma}(\omega) + \sum K_{pq\sigma,rs\tau}\delta P_{rs\tau}(\omega)\right]\,, \tag{1.39}$$

or

$$\sum_{rs\tau}^{n_{p\sigma}\neq n_{q\sigma}} \left[\delta_{\sigma,\tau}\delta_{p,r}\delta_{q,s}\frac{\omega - (\epsilon_{p\sigma} - \epsilon_{q\sigma})}{n_{q\sigma} - n_{p\sigma}} - K_{pq\sigma,rs\tau}\right]\delta P_{rs\tau}(\omega) = b_{pq\sigma}(\omega)\,. \tag{1.40}$$

We can solve this equation at each frequency ω and so calculate the response of each property a at that frequency. But we would like to go further and have an SOS-type formula so that we can extract excitation energies and their associated oscillator strengths.

After some algebra and assuming occupation numbers equal to 0 or 1 and real orbitals, it can be shown [2] that Eq. (1.40) can be rewritten as,

$$\left\{\omega \begin{bmatrix} -\boldsymbol{1} & \boldsymbol{0} \\ \boldsymbol{0} & +\boldsymbol{1} \end{bmatrix} - \begin{bmatrix} \boldsymbol{A} & \boldsymbol{B} \\ \boldsymbol{B}^* & \boldsymbol{A}^* \end{bmatrix}\right\} \begin{pmatrix} \delta\mathbf{P}(\omega) \\ \delta\mathbf{P}^*(\omega) \end{pmatrix} = \begin{pmatrix} \mathbf{b}(\omega) \\ \mathbf{b}^*(\omega) \end{pmatrix}, \tag{1.41}$$

where

$$\begin{aligned} A_{ia\sigma,jb\tau} &= \delta_{\sigma,\tau}\delta_{i,j}\delta_{a,b}(\epsilon_{a\sigma} - \epsilon_{i\sigma}) + K_{ia\sigma,jb\tau} \\ B_{ia\sigma,jb\tau} &= K_{ia\sigma,bj\tau}\,. \end{aligned} \tag{1.42}$$

(Matrices have been distinguised from vectors by putting the matrices in bold italic.)

At an excitation frequency, the response the density matrix is infinite even if the perturbation is finite. This means that the excitation frequency must satisfy the pseudo-eigenvalue problem,

$$\begin{bmatrix} \boldsymbol{A} & \boldsymbol{B} \\ \boldsymbol{B} & \boldsymbol{A} \end{bmatrix} \begin{pmatrix} \mathbf{X}_I \\ \mathbf{Y}_I \end{pmatrix} = \omega_I \begin{bmatrix} +\boldsymbol{1} & \boldsymbol{0} \\ \boldsymbol{0} & -\boldsymbol{1} \end{bmatrix} \begin{pmatrix} \mathbf{X}_I \\ \mathbf{Y}_I \end{pmatrix}. \tag{1.43}$$

One way to solve this equation is to rewrite it as a true eigenvalue problem, $\Omega\mathbf{F}_I = \omega_I^2\mathbf{F}_I$, where $\Omega = (\boldsymbol{A}-\boldsymbol{B})^{1/2}(\boldsymbol{A}+\boldsymbol{B})(\boldsymbol{A}-\boldsymbol{B})^{1/2}$ and $\mathbf{F}_I = (\boldsymbol{A}-\boldsymbol{B})^{-1/2}(\mathbf{X}_I+\mathbf{Y}_I)$. This still leads to eigenvalue problems which rapidly become too large to solve by ordinary means. However the lowest several eigenvalues and eigenvalues may be solved using the iterative block Davidson Krylov space method [59, 60, 61, 62]. These iterations are usually plainly evident in the output of programs performing LR-TDDFT calculations. Oscillator strengths may be calculated using the formula [10],

$$f_I = \frac{2}{3}\sum_{q=x,y,z} |\mathbf{q}^\dagger(\boldsymbol{A}-\boldsymbol{B})^{1/2}\mathbf{F}|^2\,. \tag{1.44}$$

1.3.3 TDA-TDDFT

The Tamm-Dancoff approximation (TDA) to the linear response equation is

$$\boldsymbol{A}\mathbf{X}_I = \omega_I\mathbf{X}_I\,. \tag{1.45}$$

The TDA often gives results which are a good approximation to full LR-TDDFT results around the equilibrium geometry of the molecule with somewhat less computational effort (especially for hybrid functionals.) However we lose the polarizablity sum rule [Eq. (1.33)] and the Thomas-Reiche-Kühn (TRK) sum rule, which says that the oscillator strengths sum to the number of electrons in the system, $\sum_I f_I = N$. These are perhaps not such a great loss since we rarely have a complete set of oscillator strengths (even in a finite basis calculation) to use in the sum-over-states expression for the dynamic polarizability. Also the TRK sum rule is only strictly valid in the limit of a complete basis set and TRK basis set requirements are not the same in practice as those needed to calculate polarizabilities and excitation spectra [4].

Most importantly the TDA actually seems to give *better* excited-state potential energy surfaces than does a full linear-response calculation [63, 30, 64]. While this may seem strange for an "approximation," the reason for this better behavior is that the quality of the excitation energies obtained

in response theory depends upon the quality of the description of the ground state problem which in DFT depends in turn on the quality of the xc-functional and there can be problems with the xc-functional for the ground state. In particular, broken symmetry solutions should not occur for ground states which are closed-shell singlets when the xc-functional is exact but do occur for approximate xc-functionals. In the later case, there is a theorem [30] which says that one of the triplet LR-TDDFT excitation energies will go to zero and then become imaginary at geometries where symmetry breaking occurs. The TDA circumvents this "triplet instability problem" by decoupling the excited-state problem from the ground-state problem. Exactly how this happens is difficult to see in TDDFT except by direct calculation but is easy to understand in TDHF. That is because TDA-TDHF is the same as CIS which, as a variational method, forbids collapse of the excitation energies to unphysical values.

1.3.4 Analytic Gradients

An important aspect of quantum chemistry is the ability to calculate analytic gradients, permitting automatic geometry optimizations and providing on-the-fly forces for *ab initio* molecular molecular dynamics calculations. Developping the mathematics necessary to implement these for conventional quantum chemistry methods has been a considerable *tour de force* which is described at length in Ref. [65]. This work has been paralleled for DFT and the basic methodology for the computation of TDDFT analytic gradients has now been implemented in a number of codes [66, 67, 68, 69, 70, 71, 72]. I describe the basic ideas briefly here for TDA-TDDFT calculations which in any event is the method I recommend for calculating excited-state PESs.

We want to take analytic derivatives of excited-state energies with respect to a parameter which we will call η, and the most important example of η is a geometric parameter associated with a force. The excited state energy can be written as, $E_I = E_0 + \hbar\omega_I$, hence $\partial E_I/\partial\eta = \partial E_0/\partial\eta + \hbar\partial\omega_I/partial\eta$. Thus we need to be able to take analytic derivatives of both the ground state and of the TDA excitation energy. We will not separate space and spin in this subsection.

In quantum chemistry calculations, the molecular orbitals (MOs), ψ_s, are expanded in a basis of atomic orbitals (OAs), χ_μ: $\psi_s(\mathbf{r}) = \sum_\mu \chi_\mu(\mathbf{r})c_{\mu,s}$. (In this subsection, the MO indices include spin.) When the parameter η varies, the AOs, χ_μ, and the MO coefficients in the AO basis, $c_{\mu,s}$, both vary. We would like to separate these two types of η-dependent variations and, if possible, eliminate any derivatives with respect to the $c_{\mu,s}$ since these are costly to calculate. To carry out our program we develop, $\partial\psi_s/\partial\eta = \psi_s^\eta + \sum_\mu \psi_r U_{r,s}^\eta$. In general, the superscript η is reserved for a derivative over AOs at constant $c_{\mu,s}$ giving so-called "core" or "skeleton" terms. So, $\psi_s^\eta = \sum_\mu(\partial\chi_\mu/\partial\eta)c_{\mu,s}$. However an exception is the matrix $\mathbf{U}^\eta$ of coupled perturbed coefficients which is defined by, $\sum_\nu \chi_\nu \partial c_{\nu,s}/\partial\eta = \sum_r \psi_r U_{r,s}^\eta$. It follows that, $U_{r,s}^\eta = \sum_{\mu,\nu} c_{\mu,r}^* S_{\mu,\nu}\partial c_{\nu,s}/\partial\eta$, where, $S_{\mu,\nu} = \langle\chi_\mu|\chi_\nu\rangle$, is the AO overlap matrix. Taking the functional derivative of the MO orthonormality relation, $\delta_{r,s} = \langle\psi_r|\psi_s\rangle = \sum_{\mu,\nu} c_{\mu,r}^* S_{\mu,\nu} c_{\nu,s}$, leads to what I call the "turnover rule," $U_{q,p}^{\eta,*} = -U_{p,q}^\eta - S_{p,q}^\eta$. For real coupled perturbed coefficients, $U_{p,p}^\eta = -S_{p,p}^\eta/2$.

It is now straightforward to take the derivative of the energy expression to obtain, $\partial E/\partial\eta = E^\eta - \sum_{\mu,\nu} S_{\mu,\nu}^\eta W_{\nu,\mu}$, where, $W_{\mu,\nu} = \sum_i c_{\mu,i}\epsilon_i n_i c_{\nu,i}^*$ is the energy-weighted density matrix. The first term is the Hellmann-Feynman force. In wave function terms, $E^\eta = \langle\Psi|(\partial\hat{H}/\partial\eta)|\Psi\rangle$. The second term is the Pulay force. It is there because the AOs move with the nuclei and it is necessary to ensure that the calculated forces are zero when the calculated energy is a minimum. Since the coupled perturbed coefficients do not enter into the calculation of the first analytic derivative, the calculation of this derivative is finally really relatively trivial.

Second analytical derivatives for the ground state (not discussed here) and first analytical deriva-

tives of the TDA-TDDFT excitation energies require us to solve a coupled perturbed equation for the $U^{\eta}_{p,q}$. Recognizing that,

$$\frac{\partial P_{q,p}}{\partial \eta} = U^{\eta}_{q,p} n_p + U^{\eta,*}_{p,q} n_q = U^{\eta}_{q,p}(n_p - n_q) - S_{q,p} n_q \,, \tag{1.46}$$

we should anticipate an equation similar to the LR-TDDFT equations already found. This is indeed the case for, instead of Eq. (1.40), we find upon differentiating the MO eigencondition, $F_{p,q} = \delta_{p,q}\epsilon_q$, that,

$$\sum \left(\delta_{p,p'}\delta_{q,q'} \frac{\epsilon_q - \epsilon_p}{n_q - n_p} + K_{pq,p'q'} \right) (n_{q'} - n_{p'}) U^{\eta}_{p',q'} = F^{\eta}_{p,q} - S^{\eta}_{p,q}\epsilon_q - \sum K_{pq,p'q'} n_{p'} S^{\eta}_{p',q'} \,. \tag{1.47}$$

However it is clear from the turnover rule that there are many linear-dependencies among the coupled pertubed coefficients. By working a little harder, we arrive at the equation,

$$\sum \mathcal{A}_{ai,bj} U^{\eta}_{bj} = \mathcal{B}^{0}_{ai} \,, \tag{1.48}$$

for the nonredundant coupled perturbed coefficients, where

$$\begin{aligned} \mathcal{A}_{ai,bj} &= \delta_{i,j}\delta_{a,b} \frac{\epsilon_i - \epsilon_a}{n_i - n_a} - (K_{ai,jb} + K_{ai,bj}) \\ \mathcal{B}^{0}_{ai} &= F^{\eta}_{ai} - S^{\eta}_{ai}\epsilon_i - \sum K_{ai,kj} S^{\eta}_{jk} \,, \end{aligned} \tag{1.49}$$

and I am using the MO index convention,

$$\underbrace{abc\cdots fgh}_{unoccupied}\,\underbrace{ijklmn}_{occupied}\,\underbrace{opq\cdots xyz}_{free} \,. \tag{1.50}$$

The redundant coupled perturbed coefficients may be calculated from the nonredundant coefficients by using the expression,

$$U^{\eta}_{p,q} = \frac{1}{\epsilon_q - \epsilon_p} \left[F^{\eta}_{p,q} - S^{\eta}_{p,q}\epsilon_q - \sum K_{pq,jk} S^{\eta}_{jk} + \sum (K_{pq,bj} + K_{pq,jb}) U^{\eta}_{bj} \right] \,. \tag{1.51}$$

It follows from the eigencondition (1.45) that the derivative of the TDA-TDDFT excitation energy is, $\partial\omega/\partial\eta = \sum X^{*}_{ia}(\partial A_{ia,bj}/\partial\eta) X_{jb}$. This can be further developped as,

$$\frac{\partial \omega}{\partial \eta} = \omega^{\eta} - \sum M_{kl} S^{\eta}_{kl} + \sum L_{ck} U^{\eta}_{ck} \,, \tag{1.52}$$

where,

$$\begin{aligned} M_{kl} &= \sum X^{*}_{ia} X_{jb} \left(K_{ab,kl} - K_{ji,kl} - G_{ia,bj,kl} \right) S^{\eta}_{kl} \\ L_{ck} &= \sum X^{*}_{ia} X_{jb} \left[(K_{ab,kc} + K_{ab,ck}) - (K_{ji,kc} + K_{ji,ck}) + (G_{ia,jb,ck} + G_{ia,bj,kc}) \right] U^{\eta}_{ck} \,. \end{aligned} \tag{1.53}$$

These are the same as for CIS except for the appearance of the term, $G_{pq,p'q',p"q"} = (\partial K_{pq,p'q'}/\partial P_{p"q"})$, which is zero in CIS but involves a triple functional derivative of the xc-functional in TDDFT.

Direct implementation of Eq. (1.52) for calculation of geometric derivatives implies the solution of the coupled perturbed equation (1.48) for each geometric degree of freedom. As this would rapidly become prohibatively expensive, it is fortunate that the coupled pertubed coefficients can be replaced

Table 1.2: Summary of formulae within the two-orbital model (Fig. 1.3). I_i is minus the ionization potential of orbital i. A_a is minus the electron affinity of orbital a. $A_a(i^{-1})$ is minus the electron affinity of orbital a for the ion formed by removing an electron from orbital i. ω_T, ω_S, and ω_M are, respectively, $i \rightarrow a$ excitation energies to the triplet, singlet, and mixed symmetry states. ΔSCF quantities are obtained by the usual multiplet sum procedure [73] except that a truncated Taylor expansion of the xc-functional has been used in the DFT case. [63] The identification of I_i and A_a in the TDDFT case is based upon OEP theory (Sec. 1.2.)

Δ SCF Hartree-Fock	CIS (TDA-TDHF)
$I_i = \epsilon_i$	$I_i = \epsilon_i$
$A_a = \epsilon_a$	$A_a = \epsilon_a$
$A_a(i^{-1}) = A_a - (aa\|f_H\|ii) + (ai\|f_H\|ia)$	$A_a(i^{-1}) = A_a - (aa\|f_H\|ii) + (ai\|f_H\|ia)$
$\omega_M = \epsilon_a - \epsilon_i - (aa\|f_H\|ii) + (ai\|f_H\|ia)$	$\omega_M = \epsilon_a - \epsilon_i - (aa\|f_H\|ii) + (ai\|f_H\|ia)$
$\omega_T = \omega_M - (ia\|f_H\|ai)$	$\omega_T = \omega_M - (ia\|f_H\|ai)$
$\omega_S = \omega_M + (ia\|f_H\|ai)$	$\omega_S = \omega_M + (ia\|f_H\|ai)$
linearized ΔSCF DFT	TDA-TDDFT
$I_i = \epsilon_i - \frac{1}{2}(ii\|f_H + f_{xc}^{\uparrow,\uparrow}\|ii)$	$I_i = \epsilon_i$
$A_a = \epsilon_a + \frac{1}{2}(aa\|f_H + f_{xc}^{\uparrow,\uparrow}\|aa)$	$A_a = \epsilon_a + (aa\|f_H\|ii) + (ai\|f_{xc}^{\uparrow,\uparrow}\|ia)$
$A_a(i^{-1}) = A_a - (aa\|f_H + f_{xc}^{\uparrow,\uparrow}\|ii)$	$A_a(i^{-1}) = A_a - (aa\|f_H\|ii) + (ai\|f_H\|ia)$
$\omega_M = \epsilon_a - \epsilon_i + \frac{1}{2}(aa-ii\|f_H + f_{xc}^{\uparrow,\uparrow}\|aa-ii)$	$\omega_M = \epsilon_a - \epsilon_i + (ai\|f_H + f_{xc}^{\uparrow,\uparrow}\|ia)$
$\omega_T = \omega_M + (aa\|f_{xc}^{\uparrow,\uparrow} - f_{xc}^{\uparrow,\downarrow}\|ii)$	$\omega_T = \omega_M - (ia\|f_H + f_{xc}^{\uparrow,\downarrow}\|ai)$
$\omega_S = \omega_M - (aa\|f_{xc}^{\uparrow,\uparrow} - f_{xc}^{\uparrow,\downarrow}\|ii)$	$\omega_S = \omega_M + (ia\|f_H + f_{xc}^{\uparrow,\downarrow}\|ai)$

by a Z-vector defined implicitly by, $\sum L_{ck} U_{ck}^{\eta} = \sum Z_{ck} \mathcal{B}_{ck}^{0}$, and explicitly by solving the new coupled perturbed equation, $\sum \mathcal{A}_{ai,bj} Z_{bj} = L_{ai}$. This is a great saving because this new coupled perturbed equation is independent of the perturbation η and so need only be solved once for each geometry.

The difference between the reduced density matrix for the Ith excited state and the ground state is given by,

$$\gamma_{p,q}^{I} - \gamma_{p,q}^{0} = \frac{\partial \omega_I}{\partial h_{q,p}} = \begin{cases} -\sum X_{pa}^{*} X_{qa} & ; \quad p,q \text{ both occupied} \\ +\sum X_{iq}^{*} X_{ip} & ; \quad p,q \text{ both unoccupied} \\ Z_{p,q} & ; \quad \text{otherwise} \end{cases}, \tag{1.54}$$

This allows the calculation of excited-state properties such as true dipole moments, rather than just transition dipole moments, showing that such properties are also accessible from TDDFT. In the past, some programs have made an approximation when calculating excited-state properties by neglecting the Z-vector contribution to the excited-state reduced density matrix.

1.4 Example: Oxirane

Our recent work [64, 74] aimed at making TDDFT a viable tool for photodynamics calculations is briefly reviewed here as an application of TDDFT. Some of the calculations are routine "safe" applications, meaning that we are avoiding the known main problems of present-day TDDFT, namely: (i) the underestimation of the ionization threshold [75, 76], (ii) the underestimation of charge transfer excitation energies [77, 63, 78], and (iii) the lack of explicit two- and higher-electron excitations [2, 8, 9, 10]. In contrast, the study of photochemical pathways is a demanding application for

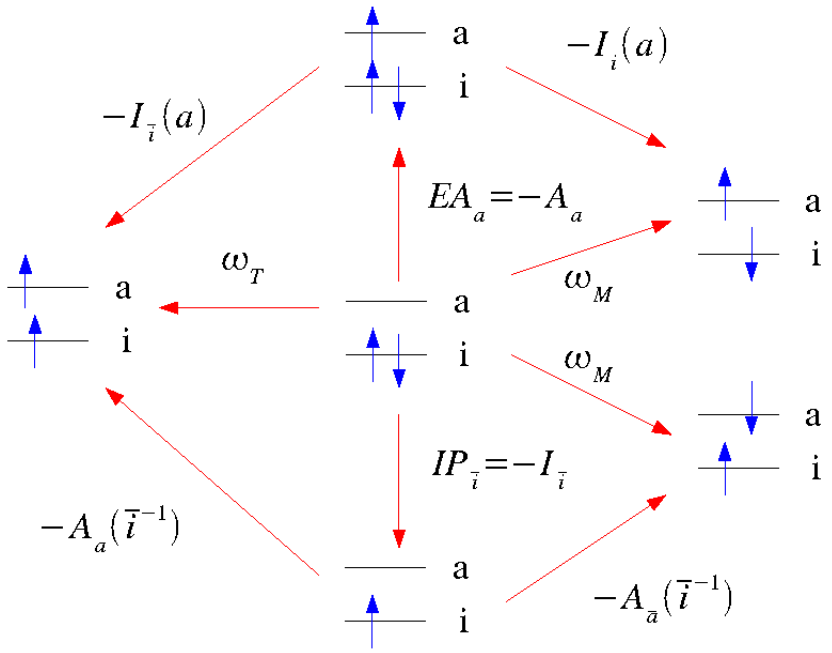

Figure 1.3: Two-orbital model.

TDDFT because of the apparent need for a coherent simultaneous description of several potential energy surfaces (PESs) over a wide range of geometries which typically involve either or both the formation of biradicaloid intermediates and charge transfer. Nevertheless TDDFT has a place in the photochemical modeler's toolbox – on condition that other methods such as complete active space self-consistant field (CASSCF) calculations be used to validate and refine results from TDDFT for the more difficult parts of photochemical processes. Viewed this way, our objective is to reduce the need to fall back onto these more expensive traditional methods. The photochemical ring opening of oxirane has been chosen for troubleshooting TDDFT photodynamics calculations because it is a small enough molecule that we can carry out very high quality comparison calculations and because it was felt that to be a simple case where TDDFT "ought to work."

Figure 1.4 shows the generally high quality to be expected of geometries optimized by DFT,

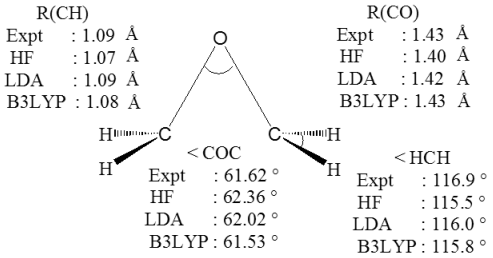

Figure 1.4: Geometric parameters for oxirane obtained from Hartree-Fock (HF), pure DFT (LDA), and hybrid DFT (B3LYP) compared with experiment. Note that the structure has C_{2v} symmetry. Adapted from Ref. [64].

Table 1.3: Principal oxirane singlet excitation energies and oscillator strengths. Adapted from Ref. [64].

Principal Singlet Excitation Energies (eV) and Oscillator Strengths (in parentheses)				
TDHF	TDLDA	TDB3LYP	Expt.	Assignment[a]
9.14 (0.0007)	6.01 (0.0309)	6.69 (0.0266)	7.24(s)[b,c,d]	$1^1B_1[2b_1(n) \rightarrow 7a_1(3s)]$
9.26 (0.0050)	6.73 (0.0048)	7.14 (0.0060)	7.45(w)[c]	$2^1B_1[2b_1(n) \rightarrow 8a_1(3p_z)]$
9.36 (0.0635)	6.78 (0.0252)	7.36 (0.0218)	7.88(s)[b], 7.89(s)[c]	$2^1A_1[2b_1(n) \rightarrow 3b_1(3p_x)]$
9.56 (0.0635)	7.61 (0.0035)	7.85 (0.0052)		
9.90 (0.0478)	7.78 (0.0304)	8.37 (0.0505)		
9.93 (0.0935)	8.13 (0.0014)	8.39 (0.0168)		
8.15 (0.0405)	8.40 (0.0419)			
12.27[e]	6.40[e]	7.68[e]	10.57[f]	

[a]TDB3LYP. [b]Gas phase UV absorption spectrum [79]. [c]Obtained by a photoelectric technique [80]. [d]Gas phase UV absorption spectrum [81]. [e]Ionization threshold ($-\epsilon_{HOMO}$). [f]Ionization potential [82].

particularly for a "normal" organic molecule such as oxirane. In this case, HF underestimates CO and CH bond lengths, but overestimates the COC bond angle. DFT leads to longer CO and CH bond lengths and a smaller COC bond angle, giving results in better overall agreement with experiment.

Table 1.3 shows how the vertical stick spectrum of oxirane calculated using LR-TDHF, LR-TDLDA, and LR-TDB3LYP compares against experimental excitation energies. Neither LR-TDHF nor CIS (values not shown) is even remotely accurate enough to assign this spectrum. This is to be contrasted with the LR-TDDFT calculations, which are of comparable computational difficulty, but markedly better accuracy. Although some care must be taken not to over interpret those features of the excitation spectrum which are close to or above the artificially low LR-TDDFT ionization threshold at $-\epsilon_{HOMO}$, the TDDFT calculations are in good enough agreement with experiment to allow us to make a credible assignment of the three principal UV absorption peaks. The assignment of the LR-TDB3LYP results is shown in Table 1.3 and is in agreement with the accepted interpretation of the experimental spectrum[83].

Figure 1.5 shows a comparison of the LR-TDLDA and TDA-TDLDA C_{2v} ring opening potential energy curves of oxirane with those obtained from CASSCF and a high-quality diffusion quantum Monte Carlo (DMC) calculation. This is not the expected photochemical reaction path, but was chosen because the high symmetry facilitates analysis of the computed results. Before discussing the figure, it is worth pointing out that the manner in which the non-DFT models were constructed provides an excellent illustration of how TDDFT is often used in photochemical calculations. Analysis of TDDFT excitation energies significantly shortened the time it would otherwise take to chose the active space for CASSCF calculations. This same active space was then also used in the DMC calculations (see Ref. [64] and references therein for additional details.) The very small differences between the LR-TDLDA and TDA-TDLDA calculations for most of the states in the figure can be explained by their Rydberg nature. In the two-level model, TDA excitation energies are always larger than full LR excitation energies,

$$\omega^2_{TDA,S} - \omega^2_{LR,S} \;=\; (ai|2f_H + f_{xc}^{\uparrow,\uparrow} + f_{xc}^{\uparrow,\downarrow}|ia)^2 \geq 0$$

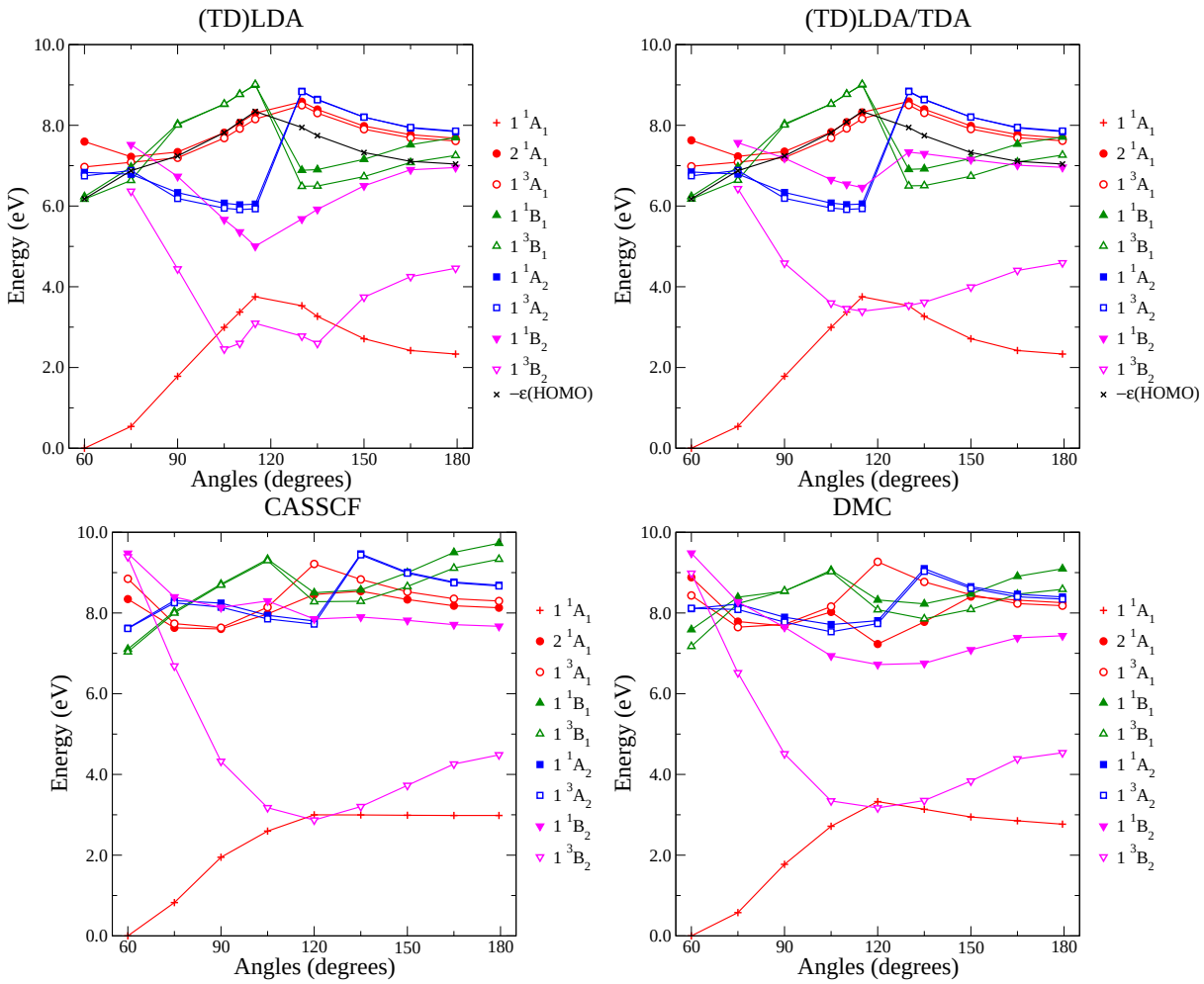

Figure 1.5: C_{2v} ring opening curves: upper left, LR-TDLDA; upper right, TDA-TDLDA; lower left, CASSCF; lower right, DMC. The energy zero has been chosen to be the ground state energy for the 60° structure. Note that the "negative excitation energies" for the LR-TDLDA 1^3B_2 state relative to the ground state are really imaginary excitation energies (triplet instability). On the other hand, the slight negative excitation energy for the TDA-TDLDA 1^3B_2 state around 120° is real. Also shown is the TDLDA ionization threshold at $-\epsilon_{HOMO}$. Adapted from Ref. [64].

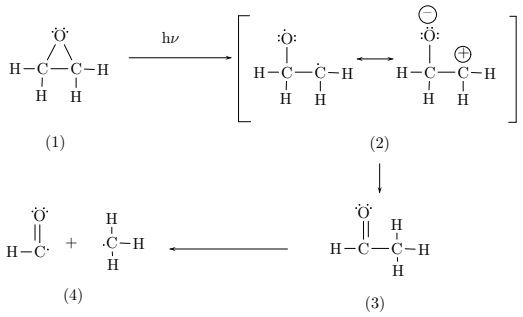

Figure 1.6: Mechanism proposed by Gomer and Noyes [84].

$$\omega^2_{TDA,T} - \omega^2_{LR,T} \;=\; (ai|f_{xc}^{\uparrow,\uparrow} - f_{xc}^{\uparrow,\downarrow}|ia)^2 \geq 0\,, \tag{1.55}$$

but the two-electron integrals are small when orbital a is diffuse. Thus the TDA and LR results are essentially identical for Rydberg states. Inspection of Table 1.2 shows that the singlet and triplet excitation energies just reduce to an orbital energy difference in this case.

Differences between the TDLDA and DMC curves are partly due to the proximity of the artificially-low TDDFT ionization threshold and partly because the quality of the LDA ground state degrades around 120°. At this point, the $6a_1(\sigma)$ HOMO interchanges with the $4b_2(\sigma^*)$ LUMO. In wavefunction terms, the quasidegenerate $6a_1^2(\sigma)$ and $4b_2^2(\sigma^*)$ states are expected to undergo an avoided crossing here in what many will recognize as the signature of the breaking of the CC σ bond to form a biradicaloid. This is exactly what happens in our CASSCF calculations where the avoided crossing is essentially described by taking a linear combination of $6a_1^2(\sigma)$ and $4b_2^2(\sigma^*)$ states. To the extent that DFT is an exact single determinant theory, exact DFT should give us the exact ground state curve without such artifices. However practical DFT uses approximate functionals and so inherits some of the problems of the structurally similar HF model. The result is that the LDA ground state curve has a cusp at around 120° (not shown because of convergence difficulties associated with a small HOMO-LUMO gap in the vicinity of this geometry.) This suggests that there should be a lower energy broken symmetry solution that mimics the underlying physics of the biradicaloid by allowing each of the CC σ electrons to localize on a different carbon. Our hypothesis is confirmed by the presence of an imaginary $^3B_2[a_1(\sigma), b_2(\sigma^*)]$ excitation eneergy in the cusp region. Notice that the energy of the associated $^1B_2[a_1(\sigma), b_2(\sigma^*)]$ is also seriously underestimated.

Symmetry breaking is not typically something one would like to do in TDDFT. Putting aside the fact that such symmetry breaking should not occur for the exact functional and that the amount of symmetry breaking can be extremly sensitive to the choice of functional (it is larger for hybrid functionals and less for the LDA and GGAs) and ignoring the fact that there may be more than one way to break symmetry in a polyatomic molecule, the main problem with symmetry breaking in TDDFT is that symmetry is very useful for assigning states. An alternative solution is simply to make the TDA. As shown in the figure the TDA-TDLDA and DMC curves for the $^3B_2$ state are in remarkably good agreement. The agreement is not as good for the $^1B_2$ state, but at least the TDA-TDLDA curve is now in the right energy range, without the need to break symmetry.

Although symmetric CC ring-opening in oxirane is not infrequently used in advanced organic chemistry courses to illustrate the application of the Woodward-Hoffmann rules for photochemical reactivity, this photochemical process is not actually observed in unsubstituted oxirane. Our recent work [74] applying mixed TDA-TDDFT/classical trajectory surface hopping dynamics [85] to oxirane recovers the experimentally-derived ring-opening mechanism of Gomer and Noyes (Fig. 1.6.)

Analysis of ring-opening trajectories shows that the $^1[n, 3p_z]$ Rydberg excitation transforms easily into a $^1[n, \sigma^*_{CO}]$ valence-type excitation, leading to facile CO bond breaking. The excited state trajectory hops to the ground state at a conical intersection which corresponds roughly to a mixed biradicaloid/carbonylide structure [(2) in Fig. 1.6.] The ground state molecule is vibrationally hot and undergoes further hydrogen transfer and CC bond breaking reactions. This also is in line with the Gomer-Noyes mechanism.

It is a fundamental tenet of chemical kinetics that experiment can never prove a mechanism, only disprove hypotheses. In contrast, our photodynamics calculation produces a mechanism, provides state-specific information about alternative pathways, and gives life-time information.

1.5 The Future

This chapter began by noting that there has been a paradigm change in quantum chemistry where DFT has almost completely replaced HF for single determinant ground-state calculations and LR-TDDFT (or TDA-TDDFT) has largely replaced LR-TDHF (or CIS) for excited-state calculations. However there has also been a paradigm change in DFT as should be evident from Sec. 1.3 on TDDFT technology – namely that DFT is taking on more and more of the aspects of traditional many-body theory. It is perhaps not too far fetched to expect that the quantum chemistry of the future will replace post-HF many-body theory calculations with post-DFT many-body theory calculations. The state-of-the-art *GW* and Bethe-Salpeter equation calculations of present day solid-state physics are certainly of this type [31]. Indeed quantum chemistry is currently expanding its frontiers to attack problems in nanoscience where reconciliation with current trends in solid-state physics theory seems both important and inevitable.

Acknowledgement

The assessment and development of TDDFT for photochemical modeling is the subject of two recent theses [86, 87]. Grenoble work on this subject continues as part of the *Réseau thématique de recherche avancée* (RTRA) project "Spectroscopy and Transport Properties in Nanomaterials: Applications and Research" and the Grenoble node of the European Theoretical Spectroscopy Facility.

Bibliography

[1] R. Singh and B. Deb, Developments in excited-state density-functional theory, Phys. Reps. **311**, 50 (1999).

[2] M. Casida, Time-dependent density-functional response theory for molecules, in *Recent Advances in Density Functional Methods, Part I*, edited by D. Chong, page 155, World Scientific, Singapore, 1995.

[3] E. Runge and E. Gross, Density functional theory for time-dependent systems, Phys. Rev. Lett. **52**, 997 (1984).

[4] C. Jamorski, M. Casida, and D. Salahub, Dynamic polarizabilities and excitation spectra from a molecular implementation of time-dependent density-functional response theory: N_2 as a case study, J. Chem. Phys. **104**, 5134 (1996).

[5] R. Bauernschmitt and R. Ahlrichs, Treatment of electronic excitations within the adiabatic approximation of time dependent density functional theory, Chem. Phys. Lett. **256**, 454 (1996).

[6] Z. Qian, A. Cconstantinescu, and G. Vignale, Solving the ultranonlocality problem in time-dependent spin-density-functional theory, Phys. Rev. Lett. **90**, 066402 (2003).

[7] M. V. Faassen, Time-dependent current-density-functional theory applied to atoms and molecules, Int. J. Mod. Phys. B **20**, 3419 (2006).

[8] R. Cave, F. Zhang, N. Maitra, and K. Burke, A dressed TDDFT treatment of the 2^1A_g states of butadiene and hexatriene, Chem. Phys. Lett. **389**, 39 (2004).

[9] N. Maitra, F. Zhang, F. Cave, and K. Burke, Double excitations within time-dependent density functional theory linear response, J. Chem. Phys. **120**, 5932 (2004).

[10] M. Casida, Propagator corrections to adiabatic time-dependent density-functional theory linear response theory, J. Chem. Phys. **122**, 054111 (2005).

[11] Y. Shao, M. Head-Gordon, and A. Krylov, The spinflip approach within time-dependent density functional theory: Theory and applications to diradicals, J. Chem. Phys. **118**, 4807 (2003).

[12] L. Slipchenko and A. Krylov, Electronic structure of the trimethylenemethane diradical in its ground and electronically excited states: Bonding, equilibrium geometries, and vibrational frequencies, J. Chem. Phys. **118**, 6874 (2003).

[13] F. Wang and T. Ziegler, Time-dependent density functional theory based on a noncollinear formulation of the exchange-correlation potential, J. Chem. Phys. **121**, 12191 (2004).

[14] Y. Tawada, T. Tsuneda, S. Yanagisawa, T. Yanai, and K. Hirao, A long-range-corrected time-dependent density functional theory, J. Chem. Phys. **120**, 8425 (2004).

[15] S. Tokura, T. Tsuneda, and K. Hirao, Long-range-corrected time-dependent density functional study on electronic spectra of five-membered ring compounds and free-base porphyrin, J. Theoretical and Computational Chem. **5**, 925 (2006).

[16] O. Vydrov and G. Scuseria, Assessment of a long-range corrected hybrid functional, J. Chem. Phys. **125**, 234109 (2006).

[17] M. Peach, E. Tellgrent, P. Salek, T. Helgaker, and D. Tozer, Structural and electronic properties of polvacetylene and polyyne from hybrid and coulomb-attenuated density functionals, J. Phys. Chem. A **111**, 11930 (2007).

[18] M. Casida and T. Wesolowski, Generalization of the Kohn-Sham equations with constrained electron density (KSCED) formalism and its time-dependent response theory formulation, Int. J. Quant. Chem. **96**, 577 (2004).

[19] T. Wesolowski, Hydrogen-bonding induced shifts of the excitation energies in nucleic acid bases: An interplay between electrostatic- and electron density overlap effects, J. Am. Chem. Soc. **126**, 11444 (2004).

[20] J. Neugebauer, M. Louwerse, E. Baerends, and T. Wesolowski, The merits of the frozen-density embedding scheme to model solvatochromic shifts, J. Chem. Phys. **122**, 094115 (2005).

[21] J. Neugebauer, Couplings between electronic transitions in a subsystem formulation of time-dependent density functional theory, J. Chem. Phys. **126**, 134116 (2007).

[22] E. Gross and W. Kohn, Time-dependent density functional theory, Adv. Quant. Chem. **21**, 255 (1990).

[23] E. Gross, C. Ullrich, and U. Gossmann, Density functional theory of time-dependent systems, in *Density Functional Theory*, edited by E. Gross and R. Dreizler, pages 149–171, Plenum, New York, 1994.

[24] E. Gross, J. Dobson, and M. Petersilka, Density-functional theory of time-dependent phenomena, Topics in Current Chemistry **181**, 81 (1996).

[25] M. Casida, Time-dependent density functional response theory of molecular systems: Theory, computational methods,and functionals, in *Recent Developments and Applications of Modern Density Functional Theory*, edited by J. Seminario, page 391, Elsevier, Amsterdam, 1996.

[26] K. Burke and E. Gross, A guided tour of time-dependent density functional theory, in *Density Functionals: Theory and Applications*, edited by D. Joubert, volume 500 of *Springer Lecture Notes in Physics*, pages 116–146, Springer, 1998.

[27] R. van Leeuwen, Key concepts in time-dependent density-functional theory, Int. J. Mod. Phys. B **15**, 1969 (2001).

[28] G. te Velde et al., Chemistry with ADF, J. Comput. Chem. **22**, 931 (2001).

[29] N. Maitra, K. Burke, H. Appel, E. Gross, and R. van Leeuwen, Ten topical questions in time-dependent density functional theory, in *Reviews in Modern Quantum Chemistry: A Celebration of the Contributions of R.G. Parr*, edited by K. Sen, pages 1186–1225, World Scientific, 2002.

[30] M. Casida, Jacob's ladder for time-dependent density-functional theory: Some rungs on the way to photochemical heaven, **828**, 199 (2002).

[31] G. Onida, L. Reining, and A. Rubio, Electronic excitations: Density-functional versus many-body Green's-function approaches, Rev. Mod. Phys. **74**, 601 (2002).

[32] C. Daniel, Electronic spectroscopy and photoreactivity in transition metal complexes, Coordination Chem. Rev. **238-239**, 141 (2003).

[33] M. Marques and E. Gross, Time-dependent density functional theory, in *A Primer in Density Functional Theory*, edited by C. Fiolhais, F. Nogueira, and M. Marques, volume 620 of *Springer Lecture Notes in Physics*, pages 144–184, Springer, 2003.

[34] M. Marques and E. Gross, Time-dependent density-functional theory, Annu. Rev. Phys. Chem. **55**, 427 (2004).

[35] K. Burke, J. Werschnik, and E. Gross, Time-dependent density functional theory: Past, present and future, J. Chem. Phys. **123**, 062206 (2005).

[36] A. Dreuw and M. Head-Gordon, Single-reference *ab initio* methods for the calculation of excited states of large molecules, Chem. Rev. **105**, 4009 (2005).

[37] M. Marques, C. Ullrich, F. Nogueira, A. Rubio, and E. Gross, editors, *Time-Dependent Density-Functional Theory*, volume 706 of *Lecture Notes in Physics*, Springer, Berlin, 2006.

[38] A. Castro et al., Octopus: a tool for the application of time-dependent density functional theory, Physica Status Solidi **243**, 2465 (2006).

[39] P. Elliott, K. Burke, and F. Furche, Excited states from time-dependent density functional theory, arXiv:cond-mat/0703590v1 22 Mar 2007.

[40] P. Hohenberg and W. Kohn, Inhomogenous electron gas, Phys. Rev. **136**, B864 (1964).

[41] Molecular spectra are not stick spectra because they include broadening for a number of reasons, including but not limited to vibrational structure. However oscillator strengths can be related to the Beer's law extinction coefficient, $\epsilon(\omega)$, by $f_I = [(m_e c \ln(10))/(2\pi^2 N_A e^2)] \int \epsilon(\omega)\, d\omega$, in Gaussian electromagnetic units, where the integration is only over spectral features arising from the electronic excitation to the Ith electronic excited state.

[42] A functional is just a function of a function. It is designated with square brackets to distinguish it from ordinary functions of numbers which are designated by parentheses.

[43] M. Levy and J. Perdew, The constrained-search formulation of density functional theory, in *Density Functional Methods in Physics*, edited by R. Dreizler and J. da Providencia, page 11, Plenum, 1985.

[44] W. Kohn and L. Sham, Self-consistent equations including exchange and correlation effects, Phys. Rev. **140**, A1133 (1965).

[45] The functional derivative of the functional $F[\rho]$ is defined by, $F[\rho + \delta\rho] - F[\rho] = \int (\delta F[\rho]/\delta\rho(\mathbf{r}))\,\delta\rho(\mathbf{r})\,d\mathbf{r}$, for arbitrary infinitessimal variations, $\delta\rho(\mathbf{r})$. This definition may be compared with the more familiar definition of a partial derivative from multivariable calculus, $f(\mathbf{v} + d\mathbf{v}) - f(\mathbf{v}) = \sum_i (\partial f(\mathbf{v})/\partial v_i) dv_i$. The essential difference is that the sum over discrete indices has been replaced by an integral over a continuous index.

[46] W. Koch and M. Holthausen, *A Chemist's Guide to Density Functional Theory*, Wiley-VCH, New York, 2000.

[47] S. Sousa, P. Fernandes, and M. Ramos, General performance of density functionals, J. Phys. Chem. A **111**, 10439 (2007).

[48] A. Becke, A new mixing of Hartree-Fock and local density functional theories, J. Chem. Phys. **93**, 1372 (1993).

[49] S. Grimme and F. Neese, Double-hybrid density functional theory for excited electronic states of molecules, J. Chem. Phys. **127**, 154116 (2007).

[50] R. Sharp and G. Horton, A variational approach to the unipotential many-electron problem, Phys. Rev. **90**, 317 (1953).

[51] J. Talman and W. Shadwick, Optimized effective atomic central potential, Phys. Rev. A **14**, 36 (1976).

[52] J. Krieger, T. Li, and G. Iafrate, Recent developments in Kohn-Sham theory for orbital-dependent exchange-correlation energy functionals, in *Density Functional Theory*, edited by E. Gross and R. Dreizler, page 91, Plenum, New York, 1995.

[53] S. Hamel, P. Duffy, M. Casida, and D. Salahub, Kohn-Sham orbitals and orbital energies: Fictitious constructs but good approximations all the same, J. Electr. Spectr. and Related Phenomena **123**, 345 (2002).

[54] X. Gonze and M. Scheffler, Exchange and correlation kernels at the resonance frequency: Implications for excitation energies in density-functional theory, Phys. Rev. Lett. **82**, 4416 (1999).

[55] R. van Leeuwen and E. Baerends, Exchange-correlation potential with correct asymptotic behavior, Phys. Rev. A **49**, 2421 (1994).

[56] S. Hamel, M. Casida, and D. Salahub, Exchange-only optimized effective potential for molecules from resolution-of-the-identity techniques: Comparison with the local density approximation, with and without asymptotic correction, J. Chem. Phys. **116**, 8276 (2002).

[57] S. Hirata, C. Zhan, E. Apra, T. Windus, and D. Dixon, A new, self-contained asymptotic correction scheme to exchange-correlation potentials for time-dependent density functional theory, J. Phys. Chem. A **107**, 10154 (2003).

[58] C. Ullrich and I. Tokatly, Nonadiabatic electron dynamics in time-dependent density-functional theory, Phys. Rev. B **73**, 235102 (2006).

[59] E. Davidson, The iterative calculation of a few of the lowest eigenvalues and corresponding eigenvectors of large real-symmetric matrices, J. Comput. Phys. **17**, 87 (1975).

[60] C. Murray, S. Racine, and E. Davidson, Improved algorithms for the lowest few eigenvalues and eigenvectors of large matrices, J. Comput. Phys. **103**, 382 (1991).

[61] J. Olsen, H. Jensen, and P. Joergensen, Solution of the large matrix equations which occur in response theory, J. Comput. Phys. **74**, 265 (1988).

[62] R. Stratmann, G. Scuseria, and M. Frisch, An efficient implementation of time-dependent density-functional theory for the calculation of excitation energies of large molecules, J. Chem. Phys. **109**, 8218.

[63] M. Casida et al., Charge-transfer correction for improved time-dependent local density approximation excited-state potential energy curves: Analysis within the two-level model with illustration for H_2O and LiH, J. Chem. Phys. **113**, 7062 (2000).

[64] F. Cordova et al., Troubleshooting time-dependent density-functional theory for photochemical applications: Oxirane, J. Chem. Phys. **127**, 164111 (2007).

[65] Y. Yamaguchi, Y. Osamura, J. Goddard, and H. S. III, *A New Dimension to Quantum Chemistry: Analytic Derivative Methods in* Ab Initio *Molecular Electronic Structure Theory*, Oxford University Press, Oxford, 1994.

[66] C. V. Caillie and R. Amos, Geometric derivatives of excitation energies using SCF and DFT, Chem. Phys. Lett. **308**, 249 (1999).

[67] C. V. Caillie and R. Amos, Geometric derivatives of density functional theory excitation energies using gradient-corrected functionals, Chem. Phys. Lett. **317**, 159 (2000).

[68] F. Furche and R. Ahlrichs, Adiabatic time-dependent density functional methods for excited state properties, J. Chem. Phys. **117**, 7433 (2002).

[69] D. Rappoport and F. Furche, Analytical time-dependent density functional derivative methods within the RI-J approximation, an approach to excited states of large molecules, J. Chem. Phys. **122**, 064105 (2005).

[70] J. Hutter, Excited state nuclear forces from the Tamm-Dancoff approximation to time-dependent density functional theory within the plane wave basis set framework, J. Chem. Phys. **118**, 3928 (2003).

[71] N. Doltsinis and D. Kosov, Plane wave/pseudopotential implementation of excited state gradients in density functional linear response theory: A new route via implicit differentiation, J. Chem. Phys. **122**, 144101 (2005).

[72] G. Scalmani et al., Geometries and properties of excited states in the gas phase and in solution: Theory and application of a time-dependent density functional theory polarizable continuum model, J. Chem. Phys. **124**, 094107 (2006).

[73] T. Ziegler, A. Rauk, and J. Baerends, Calculation of multiplet energies by Hartree-Fock-Slater method, Theor. Chim. Acta **43**, 261 (1977).

[74] E. Tapavicza, I. Tavernelli, U. Röthlisberger, C. Filippi, and M. Casida, Mixed time-dependent density-functional theory/classical trajectory surface hopping study of oxirane photochemistry, in preparation.

[75] M. Casida, C. Jamorski, K. Casida, and D. Salahub, Molecular excitation energies to high-lying bound states from time-dependent density-functional response theory: Characterization and correction of the time-dependent local density approximation ionization threshold, J. Chem. Phys. **108**, 4439 (1998).

[76] M. Casida, K. Casida, and D. Salahub, Excited-state potential energy curves from time-dependent density-functional theory: A cross-section of formaldehyde's $^1A_1$ manifold, Int. J. Quant. Chem. **70**, 933 (1998).

[77] D. Tozer, R. Amos, N. Handy, B. Roos, and L. Serrano-Andrés, Does density functional theory contribute to the understanding of excited states of unsaturated organic compounds?, Mol. Phys. **97**, 859 (1999).

[78] A. Dreuw, J. Weisman, and M. Head-Gordon, Long-range charge-transfer excited states in time-dependent density functional theory require non-local exchange, J. Chem. Phys. **119**, 2943 (2003).

[79] T.-K. Liu and A. Duncan, The absorption spectrum of ethylene oxide in the vacuum ultraviolet, J. Chem. Phys. **17**, 241 (1949).

[80] A. Lowrey III and K. Watanabe, Absorption and ionization coefficients of ethylene oxide, J. Chem. Phys. **28**, 208 (1958).

[81] G. Fleming, M. Anderson, A. Harrison, and L. Pickett, Effect of ring size on the far ultraviolet absorption and photolysis of cyclic ethers, J. Chem. Phys. **30**, 351.

[82] W. von Niessen, L. Cederbaum, and W. Kraemer, The electronic structure of molecules by a many-body approach VIII. Ionization potentials of the three-membered ring molecules C_3H_6, C_2H_4O, C_2H_5N, Theor. Chim. Acta **44**, 85 (1977).

[83] H. Basch, M. Robin, N. Kuebler, C. Baker, and D. Turner, Optical and photoelectron spectra of small rings. III. The saturated three-membered rings, J. Chem. Phys. **51**, 52 (1969).

[84] E. Gomer and J. W. A. Noyes, Photochemical studies. XLII. Ethylene oxide, J. Am. Chem. Soc. **72**, 101 (1950).

[85] E. Tapavicza, I. Tavernelli, and U. Röthlisberger, Trajectory surface hopping within linear response time-dependent density-functional theory, Phys. Rev. Lett. **98**, 023001 (2007).

[86] F. Cordova, *Photochemistry from Density-Functional Theory*, PhD thesis, Université Joseph Fourier (Grenoble I), Grenoble, France, 2007.

[87] E. Tapavicza, *Nonadiabatic First Principles Molecular Dynamics: Development and Applications to Photochemistry*, PhD thesis, École Polytechnique Fédérale de Lausanne, Lausanne, Switzerland, 2008.